Review

# Photocatalytic degradation using design of experiments: A review and example of the Congo red degradation

Vasilios A. Sakkas*, Md. Azharul Islam, Constantine Stalikas, Triantafyllos A. Albanis

*Department of Chemistry, University of Ioannina, Panepistimioupolis, Ioannina 45110, Greece*

## ARTICLE INFO

## ABSTRACT

The use of chemometric methods such as response surface methodology (RSM) based on statistical design of experiments (DOEs) is becoming increasingly widespread in several sciences such as analytical chemistry, engineering and environmental chemistry. Applied catalysis, is certainly not the exception. It is clear that photocatalytic processes mated with chemometric experimental design play a crucial role in the ability of reaching the optimum of the catalytic reactions. The present article reviews the major applications of RSM in modern experimental design combined with photocatalytic degradation processes. Moreover, the theoretical principles and designs that enable to obtain a polynomial regression equation, which expresses the influence of process parameters on the response are thoroughly discussed. An original experimental work, the photocatalytic degradation of the dye Congo red (CR) using $TiO_2$ suspensions and $H_2O_2$, in natural surface water (river water) is comprehensively described as a case study, in order to provide sufficient guidelines to deal with this subject, in a rational and integrated way.

© 2009 Elsevier B.V. All rights reserved.

## Contents

## 1. Introduction

Quality problems of groundwater and freshwater, have generated several studies in last years dealing with catalytic water treatment processes, called advanced oxidation processes (AOPs). These chemical-oxidative processes, are characterized by the generation of hydroxyl radicals, one of the strongest known oxidant. Therefore, it is possible for the hydroxyl radical to oxidize and mineralize almost every organic molecule into $CO_2$ and inorganic ions. AOPs such as $H_2O_2$/UV processes, Fenton and photo-Fenton catalytic reactions [1–3] and $TiO_2$ mediated photocatalysis [4–6] have been widely used to destroy organic pollutants including pharmaceutical active compounds (PhACs) and personal care products (PCPs) [7–10].

Heterogeneous photocatalysis takes advantage of semiconducting metal oxides that can be used on photo-assisted reactions either suspended in the water effluent to be treated, or immobilized on various types of supports. $TiO_2$-based photocatalysis appears as the most emerging destructive technology. The key advantage of the former is that it can be carried out under ambient conditions (atmospheric oxygen is used as oxidant) and may lead to complete mineralization of organic carbon into $CO_2$. Moreover, $TiO_2$ photocatalyst is largely available, inexpensive, non-toxic and shows relatively high chemical stability. Finally, the $TiO_2$ photocatalytic process, is receiving increasing attention because of its low cost when using sunlight as the source of irradiation.

The utilization of combined photocatalysis and solar technologies may be developed to a useful process for the reduction of water pollution by micropollutants (e.g. PhACs, PCPs, pesticides and dyes) because of the mild conditions required and their efficiency in the mineralization.

In this context, the application of photocatalytic procedures for remediation have been mostly studied in terms of determination of reaction kinetics, the reaction mechanisms involved in the process as well as of the identification of major transient intermediates. Most of the studies dealing with kinetics make use of the traditional one-factor-at-a-time (OFAT) approach, examining the effect of parameters such as initial concentration of target compound, degradation time, catalyst dose and characteristics, pH, temperature, UV light source and intensity.

If the factors involved in the process are independent (which is rarely the situation), the most common practice is OFAT while holding all others constant. However, the result of this univariate analysis shows inadequate optimization towards response(s). Moreover, OFAT approach is costly in sense of time and reagents, and not that efficient. There is now increasing recognition that hereditary malpractice ought to be replaced by soundly based chemometric methods such as response surface methodology (RSM) based on statistical design of experiments (DOEs). Such statistical analyses are more efficient, since they account for interaction effects between the studied variables and determine more accurately the combination of levels that produces the optimum of the process. It is, therefore, clear that the chemometric experimental design in photocatalytic processes play crucial role in the ability of reaching the optimum of the catalytic reaction. The importance and theoretical concepts behind the optimization through experimental design as well as RSM in research and development efforts have been thoroughly discussed in a number of informative articles [11–21] and the sequential steps of RSM are also highlighted in subsequent sections of this study. According to our knowledge, there are no general monographs or reviews to emphasize the broad nature of photocatalytic processes mated with chemometrics, the wide range of approaches that can be employed and the great impact on the data obtained.

In the present study an attempt was made to emphasize on the study of a dye $TiO_2$-mediated degradation capitalizing on the potency of chemometrics. For this reason, a thorough step-by-step chemometric approach is discussed to optimize and validate the catalytic processes. At the same time, this paper reviews significant applications based on design of experiments and optimization techniques in the field of photocatalysis. Moreover, an original experimental work, with regards to photocatalytic degradation of the dye, Congo red in river water as a case study is woven into the text, giving the guidelines to deal with this subject, in a rational way.

Congo red (CR) (sodium 3,3′-(1E,1′E)-biphenyl-4,4′-diylbis (diazene-2,1-diyl)bis(4-aminonaphthalene-1-sulfonate)) is one of the most frequently used secondary diazo dye. Benzidine is a toxic metabolite of Congo red, which causes cancer of the bladder in humans [22]. Congo red effluents are highly colored, have low biological oxygen demand (BOD) and high chemical oxygen demand (COD) while they contain high amounts of dissolved solids [23].

## 2. Building a response surface methodology

### 2.1. Factor screening experiments

The first step during the development of an application, experimental work or research, in general, is the definition of the problem. Generally, the process of specifying the problem is an innately process from abstraction and approximation. Therefore, one should consider the whole procedure of designated work, including all the critical steps, raw materials, equipment, costs and time in order to obtain a holistic view of the problem. Afterwards, the selection of appropriate response(s) or output(s) is important since it should take into consideration the sources of error, ways of minimizing it and of course the ability to follow the change in response(s), in course of time.

In photocatalytic processes for example, possible response(s) could be, percent of degradation, and decolorization rate of degradation or even degree of mineralization and/or detoxification of the sample. On the other hand, variables that affect the response could be, initial concentration of target compound, illumination time, catalyst dose and/or characteristics, pH, temperature, UV irradiance, and electron acceptors. For a given photocatalytic reaction, it is difficult to infer which of the above variables would have a significant effect on the process, since their impact is interdependent.

Screening test is the most appropriate experimental procedure to discover suitable independent variables or screening out insignificant variables among others, in order to identify those that may display a significant effect on the selected response. The well-known Plackett–Burman (two-level fractional design) or full factorial design is usually employed as screening test [24].

### 2.2. The path of steepest ascent/descent

The main objective of the experimenters is to estimate the current levels of factors that are near to optimum or not. If current levels of independent variables are far from optimum conditions, then the location of the region of factor levels that produce optimal conditions is the next step. The method of steepest ascent is followed to move the experimental region of a response in the direction of the maximum change toward the optimum. On the other hand, the method of steepest descent is followed when minimum response is desired. The step size is determined usually by prior knowledge of the process, or other practical features of the studied system. The lack-of-fit test compares residual error (from model error) to pure error (from replicated experiments or from central points). If the model does not fit the data well, lack-of-fit will be significant. Besides, if significant curvature or lack-of-fit is

detected in the first-order model, a second-order model should be used for solving real response surface problems.

## 2.3. Choice of design for RSM

The most important part before applying the RSM methodology, is the selection of appropriate design of experiment (DOE), that have a large influence on the building of response surface and thus, its precision on the prediction. Simply, the purpose of DOE is the selection of the experimental points at which the response should be evaluated. The common DOEs used in RSM are.

### 2.3.1. Full three level factorial design

Three-level full factorial designs are designed, in which, factors can take on three values: low, medium or center and high. Generally, if midpoints or center points are added on $2^k$ full factorial design then it will be $3^k$ full factorial design, where $k$ is the number of factors but the main disadvantage of this design ($3^k$) is the need for large number of experimental runs, which produced unwanted, high-order interactions. Therefore, a $3^k$ full factorial design will be more appropriate if factors are less than five.

### 2.3.2. Central composite design (CCD)

CCD is the most frequently used five level fractional factorial designs for the construction of second-order response surface model. This design consists of three types of points: cube points that come from factorial design, axial points and center points, therefore total number of experiments ($N$) needed can be determined by $N = 2^k + 2k + C_0$, where $k$ is the number of factors, $2^k$ is the cubic runs, $2k$ is the axial runs and $C_0$ is the center point's runs. The center point of CCD is often used to calculate experimental error. The distance of axial points from the center points are denoted by $\alpha$ that is depend on the number of factors chosen for the experiment. The main drawback of using CCD is time consuming design with large numbers of factors.

### 2.3.3. Doehlert design

This design is for heterogeneous levels of variable that allows a free choice of the factors to be assigned to a large or a small number of levels. Besides, Doehlert design needs small number of experimental runs even with large number of factors. The number of experiments required ($N$) is given by $N = k^2 + k + C_0$, where $k$ is the number of variables and $C_0$ is the number of center points. More details about Doehlert design are also well described by several articles [15,17].

### 2.3.4. Box–Behnken design

Box–Behnken design is for three levels of variables that are evenly spaced. The number of experiments required ($N$) is given by $N = 2k(k - 1) + C_0$, where $k$ is the number of variables and $C_0$ is the number of center points. The main advantage of using Box–Behnken design is that this design avoids extreme conditions of experiments. Ferreira et al. [14] discuss the use and application of Box–Behnken design in different fields of chemistry as an optimization procedure of analytical methods.

After the selection of the appropriate experimental design, the nomination of levels of the variable should be handled carefully, based on the path of steepest ascent/descent, preliminary experiments, prior knowledge of the process attributes or literature review and certain instrumental limitations.

## 2.4. Sequential mathematical model fitting

It is important to fit a mathematical model equation in order to describe the behavior of the response in the experimental domain by selected DOE. As RSM is mainly based on second-order polynomial model, the experimenters should sequentially fit the first-order model to second-order polynomial model. The first-order model will be applicable when the approximation of true functional relationship between response and the set of independent variables has a relatively small region of interest. In other sense, first-order model uses low-order polynomial model divulging some part of the response surface. Generally, this model is appropriate for describing a flat surface, according to the equation:

$$R = \beta_0 + \sum \beta_i X_i + \varepsilon \tag{1}$$

In Eq. (1), $R$ is the response, $\beta_0$ is the constant term, $\beta_i$ represents the coefficients of the linear parameters, $X_i$ represents the variables and $\varepsilon$ is the random error or noise to the response. Sometimes, it is called main-effects model because it includes only the main effects of the variables.

If interaction terms are included (called factor interactions or FI model), the first-order model can then be represented as follows:

$$R = \beta_0 + \sum \beta_i X_i + \sum \beta_{ij} X_i X_j + \varepsilon \tag{2}$$

where $\beta_{ij}$ represents the coefficients of the interaction parameters $X_i$ and $X_j$ and $i < j$.

If first-order or FI models are not adequate to the representation of true functional relationships with independent variables, then a more highly structured, flexible and diversified functional forms model, such as second-order model, may be studied in order to locate the optimum point. The second-order model can be expressed as follows:

$$R = \beta_0 + \sum \beta_i X_i + \sum \beta_{ij} X_i X_j + \sum \beta_{ii} X_i^2 + \varepsilon \tag{3}$$

where $\beta_{ii}$ represents the coefficients of the quadratic parameter and $i < j$.

In order to determine the adequacy of the first-order and second-order model, an experimenter can opt for examining the normal plots, the residual analysis, the main and interaction effects, the contour plot, and analysis of variance (ANOVA) statistics ($F$-test, $t$-test, $R^2$, the adjusted $R^2$, and lack-of-fit).

## 2.5. Optimization

The optimization is the way of adjusting control variables in any process to find out the suitable factors levels that return the best possible outcome (response). The traditional "trial-and-error" or OFAT approach for optimization has lots of drawbacks in relation to the absence of interactions effect as well as the efficiency to predict the true optimum. Generally, there are two different strategies for optimization: (a) simplex optimization and (b) response surface methodology (RSM). Simplex optimization is a stepwise strategy of the experiments, which are performed one by one. The exception is the starting simplex, in which all experiments can be run in parallel. An exact optimum can only be determined by RSM, while the simplex method will encircle the optimum [11]. As our objective is to optimize process parameters using RSM, we will probe into this optimization methodology.

The RSM is mainly based on second-order models; so it illustrates quadratic surfaces such as minimum, maximum, ridge and saddle. If the second-order model is found to be adequate (Eq. (3)), then canonical analysis is performed to determine the location and the nature of the stationary point of the second-order model. The stationary point is the combination of design variables, where the surface is at either maximum or minimum in all directions. If the stationary point is maximum in some direction and minimum in another one, then the stationary point is a *saddle point*. When the surface is curved in one direction but is fairly constant

**Table 1**
Examples of photocatalytic degradation using RSM.

| Compound | Photocatalytic process | Selected variables | DOE and optimization techniques | Analytical instrument(s) | Ref. |
|---|---|---|---|---|---|
| Hydroxybutanedioic acid | $TiO_2$-coated fiber-optic/UV | Number of layers, coating length (cm) | $2^2$ full factorial design + 3 center points | HPLC-UV | [39] |
| Terephthalic acid | $TiO_2$ (Degussa P25)/UV | Irradiation time, $TiO_2$ concentration, terephthalic acid concentration | Three-factor central composite rotatable design | Fluorescence spectrophotometer | [40] |
| Acid Blue 7 | Nano-$TiO_2$/UV | pH, light intensity, $TiO_2$ concentration | Box–Behnken design | UV-spectrophotometer | [41] |
| Reactive Red 239 | $TiO_2$/UV | UV light intensity, the concentration of $TiO_2$, initial pH, stirring speed | $2^4$ full-factorial central composite design (CCD) | UV-spectrophotometer | [42] |
| Reactive Blue 19 | $TiO_2$/ZnO/UV | pH, amount of catalyst, dye concentration | Factorial design | Spectrophotometer | [43] |
| Indole | $TiO_2$/UV | Indole concentration, $TiO_2$ amount, temperature, flow rate | Central composite experimental design (CCD) | UV visible absorption spectrometry | [44] |
| Phenol | $TiO_2$/ZnO/UV | pH, phenol concentration, catalyst | $2^3$ factorial design | Luminescence spectrometer | [45] |
| Azo dye Metanil Yellow | $TiO_2$/UV | Dye concentration, $TiO_2$ concentration, pH, light flux | Central composite design face-centered (CCF) | UV–vis spectrophotometer | [46] |
| Phenol | $TiO_2$/UV | Catalyst ($TiO_2$) size, $TiO_2$ concentration, dissolved oxygen concentration and phenol concentration | Box–Behnken design (BBD) | HPLC | [47] |
| Acid dye | $TiO_2$ thin film/UV | According to the Plackett–Burman design, the alcohol-to-titanium ratio, the acid-to-titanium ratio, and the sol–gel reaction time | Plackett–Burman design, $2^3$ full factorial design, simplex method optimization | UV/vis spectrophotometer | [48] |
| Diuron | $H_2O_2$/Fe(II)/UV | Pesticide dose, hydrogen peroxide dose, ferrous ion dose Fe(II) | Box–Behnken design | HPLC | [49] |
| Fulvic acid | Ti/$TiO_2$/UV | pH, potassium peroxodisulphate ($K_2S_2O_8$) concentration, bias potential | Box–Behnken design | Total organic carbon analyzer (TOC) | [50] |
| Ethylenediaminetetraacetic acid (EDTA) | $TiO_2$/UV | EDTA concentration, photocatalyst concentration, pH, irradiation time | Full factorial and Doehlert experimental designs, artificial neural networks (ANNs) | UV/VIS-Absorption spectrophotometer | [51] |
| Acid Red 14 | UV/Fe-ZSM5/$H_2O_2$ | Concentration of the catalyst, molar ratio of initial concentration of $H_2O_2$ to that of the dye (H value), initial concentration of the dye and initial pH of the solution | Central composite design (CCD), artificial neural networks (ANNs) | Total organic carbon (TOC) VCSN analyzer | [52] |
| Basic Red 2(BR2) | $H_2O_2$/UV | BR2 concentration, pH and $H_2O_2$ concentration | D-optimal design | UV–vis spectrophotometer | [53] |
| Carmine (C.I. Natural Red 4) | $H_2O_2$/UV | Carmine concentration, $H_2O_2$ concentration, pH and reaction time | D-optimal design | UV–vis spectrophotometer | [54] |
| Dyeing wastewater | $TiO_2$/$H_2O_2$/UV | $TiO_2$ and $H_2O_2$ concentration | Central composite design (CCD) | UV–vis spectrophotometer | [55] |
| Orange II | $TiO_2$/$H_2O_2$/UV | $H_2O_2$ concentration | Central composite design (CCD) and then optimization through gradient method of steepest ascent | UV–vis spectrophotometer | [56] |
| Direct Red 28 | Fe(II)/$H_2O_2$/UV | Dyestuff dose (mg $L^{-1}$), hydrogen peroxide dose (mg $L^{-1}$) and ferrous ion dose (mg $L^{-1}$) | Box–Behnken design | UV–vis spectrophotometer | [57] |

Table 1 (*Continued*)

| Compound | Photocatalytic process | Selected variables | DOE and optimization techniques | Analytical instrument(s) | Ref. |
|---|---|---|---|---|---|
| Diuron and Linuron | Fe(II)/$H_2O_2$/UV | Hydrogen peroxide dose and iron concentration | Central composite design | HPLC system | [2] |
| Alachlor | Fe(II)/$H_2O_2$/UV | Temperature 20–50 °C, iron concentration 2–20 mg/L, illuminated volume 11.9–59.5% of total | Central composite design without star points | HPLC-UV | [58] |
| Phenol | US (ultrasound)/Fe-SBA-15/$H_2O_2$ | Catalyst concentration ranging from 0.2 to 1.0 g $L^{-1}$, and hydrogen peroxide concentration from 1.19 to 4.76 g $L^{-1}$ | A complete 32 full factorial experimental design | TOC Analyzer | [59] |
| 2,4-Dimethyl aniline | $Fe^{3+}$-exchanged zeolite Y/$H_2O_2$/UV | $Fe^{3+}$ concentration and $H_2O_2$ concentration | Factorial matrices $2^2$ and Doehlert matrices | HPLC | [60] |
| Cu(II) | $TiO_2$/UV | Catalyst mass, pH, and reaction time | Factorial design | Atomic absorption flame spectrophotometer | [61] |
| Tetracycline | $TiO_2$/UV and ZnO/UV | $TiO_2$ dose and pH; ZnO dose and pH | Central composite circumscribed design (CCCD) | Spectrophotometer | [62] |
| Flumequine | Pure $TiO_2$, urea TiO (u-$TiO_2$) and thiourea TiO (t-$TiO_2$)/simulated solar light | pH and catalysts dose | Central composite circumscribed design(CCCD) | Spectrophotometer and HPLC | [63] |

in another one, then this type of surface is called ridge system [25]. The visualization optimization of the predicted model equation can be obtained by the 3D surface response plot and by contour plots through determination of coordinate axes.

Desirability function is a popular and established technique to concurrently determine these settings of input variables that can give the optimum performance levels for one or more responses. Harrington [26] first developed the desirability function which was later modified by Derringer and Suich [27] for specifying the relationship between predicted responses on a dependent variable and the desirability of the responses.

The desirability is an objective function ($D$) that ranges from zero (low) outside of the limits to one (maximum) at the goal. The numerical optimization finds a point that maximizes the desirability function. The characteristics of a goal may be altered by adjusting the weight or importance of the factors based on experimenter's desire. For several responses and factors, all goals transformed into one desirability function:

$$D = (d_1 \times d_2 \times d_3, ..., d_n)^{1/n} = \left( \prod_{i=1}^{n} d_i \right)^{1/n} \tag{4}$$

where $d_i$ indicates the desirability of the response and $n$ is the number of responses in the measure. According to this, Eq. (4) can be extended to

$$D = \left[ d_1^{v1} \times d_2^{v2} \times ... \times d_n^{vn} \right]^{1/n}, \quad 0 \le v_i \le 1 \ (i = 1, 2, ..., n),$$

$$\sum_{i=1}^{n} v_i = 1 \tag{5}$$

where $d_i$ indicates the desirability of the response $y_i$ ($i = 1, 2, 3, ..., n$) and $v_i$ represents the importance of responses that varies from the least important ($v_i = 1$) to the most important ($v_i = 5$). So, the maximum overall desirability function $D$, depends on the $v_i$ (importance) value.

Other, less frequently used manners to reach optimal conditions encompass artificial neural networks (ANNs). ANNs gather their knowledge by detecting the patterns and relationships in data and learn (or are trained) through experience. They have the ability to approximate virtually any function in a stable and efficient way and, for this reason, they can be applied to quantify a nonlinear relationship between causal factors and responses by means of iterative training of data obtained from a designed experiment [19].

### 2.6. Confirmation study

The confirmation study is performed under optimized conditions and should compare this result with the predictions. If the results (response) of confirmation experiments agree with the predictions, then the developed model is robust and insensitive to external noises or tolerances by changing factors levels.

## 3. Applications of DOE in photocatalytic process

Although photocatalytic oxidation process is an emerging technology used for the destruction of hazardous compounds, in the last three decades, few reports dealing with the application of statistical design of experiments towards the photocatalytic degradation process are available. As already mentioned, the univariate or OFAT approach ignores the interactions effect of selected photocatalytic variables and provides misguided prediction of optimum photocatalytic degradation efficiency. By considering this, several researchers have followed the employment of statistical design of experiments for the photocatalytic treatment process. Having in mind to give an overview of the most relevant applications, a representative number of them are described here, while more relative studies are depicted at Table 1.

Emilio et al. [28] implemented two different experimental designs for photocatalytic degradation of nitrilotriacetic acid (NTA). A two-level full factorial design was applied to evaluate the statistical meaning of factors and their interactions through multiple-way analysis of the variance (MANOVA). Four factors were chosen, NTA

**Table 2**
Design matrix and results of two-level fractional factorial design (resolution III) with five factors for screening test.

| Range and level | | | | | | |
|---|---|---|---|---|---|---|
| Factors | | Low (−1) | | Middle (0) | | High (+1) |
| pH | | 4 | | 6 | | 8 |
| Irradiance (W/m$^2$) | | 520 | | 600 | | 680 |
| Dye concentration (mg/L) | | 50 | | 100 | | 150 |
| TiO$_2$ (mg/L) | | 700 | | 1000 | | 1300 |
| H$_2$O$_2$ (mg/L) | | 1.5 | | 5 | | 8.5 |

| Design matrix | | | | | | |
|---|---|---|---|---|---|---|
| Run | pH | Irradiance | Dye concentration | TiO$_2$ | H$_2$O$_2$ | Degradation % |
| 1 | +1 | −1 | −1 | −1 | −1 | 52.36 |
| 2 | 0 | 0 | 0 | 0 | 0 | 57.29 |
| 3 | −1 | +1 | +1 | −1 | −1 | 60.90 |
| 4 | +1 | +1 | −1 | +1 | −1 | 77.26 |
| 5 | +1 | +1 | +1 | +1 | +1 | 79.90 |
| 6 | −1 | +1 | −1 | −1 | +1 | 60.91 |
| 7 | −1 | −1 | +1 | +1 | −1 | 72.65 |
| 8 | 0 | 0 | 0 | 0 | 0 | 56.35 |
| 9 | −1 | −1 | −1 | +1 | +1 | 74.66 |
| 10 | +1 | −1 | +1 | −1 | +1 | 73.15 |

concentration, pH, TiO$_2$ concentration and time, while 24 experimental runs were applied. Based on MANOVA analysis, pH was maintained at a constant value for further study. Subsequently, a Doehlert design of 13 runs, having a greater number of levels, was used to train an ANN for optimization. From the study it has been demonstrated that NTA degradation is more efficient at low pH, while TiO$_2$/NTA concentration ratio, must be large enough to keep the reaction under a first-order regime, which provides the highest reaction rate.

In a recent study by our research group [29], CCD was employed to analyze the simultaneous effect of H$_2$O$_2$, Fe(II) and TiO$_2$ in the photocatalytic degradation of the pharmaceutical agent imipramine in aqueous solution. Experimental data were then fitted using ANNs for optimization. The findings indicated that ANN provides excellent predictive performance while the influence of each variable studied was assessed, with TiO$_2$ being the most significant factor, followed by H$_2$O$_2$ and Fe(II). In another study [9], CCD was used for the optimization of photocatalytic degradation of the pharmaceutical agent salbutamol in aqueous TiO$_2$ suspensions. In this design, 11 experiments were performed, at which the two variables (TiO$_2$ concentration and pH) were codified in five levels with three central points for statistical validity. The objective of another study [10] was the photocatalytic degradation of diclofenac using a multivariate analysis technique. Experiments were carried out according to a 2$^2$ factorial design with 10 (3 center point) experimental runs. Selected response was diclofenac residual concentration (%) after 30 min of light irradiation while TiO$_2$ concentration and diclofenac concentration were the input parameters for this case. From the response surface plot, the optimum conditions were found to be: TiO$_2$ 624 mg L$^{-1}$ and initial diclofenac concentration of 8.17 mg L$^{-1}$.

Korbahti and Rouf [30] applied RSM in order to optimize the discoloration of toludine blue, in the presence of UV radiation, using a heterogeneous hybrid V$_2$O$_5$/TiO$_2$ catalyst. The runs were designed in accordance with a D-optimal design and the independent variables being the dye concentration, pH and catalyst concentration. The design was augmented with three replications in order to evaluate the pure error. The optimum degradation conditions were found to be 26.5 mg/20 mL of V$_2$O$_5$/TiO$_2$ catalyst, at pH 7.7. In another study by the same research group [31], Rose Bengal (C.I. name is Acid Red 94) photocatalytic degradation was studied, in the presence of hydrogen peroxide. D-optimal design with six

replications was used, while dye concentration, pH and H$_2$O$_2$ concentration were chosen as input variables. This study suggested that dye decolorization increased with increasing H$_2$O$_2$ concentration.

Lin et al. [32] employed CCD based on RSM in the optimization of methylparaben photocatalytic degradation. The selected process parameters were pH, TiO$_2$ loading, oxygen concentration and light flux. The applied experimental design consisted of 28 experiments divided into three blocks: (a) four variables ($n = 4$) at two levels: low (−1) and high (+1), full factorial design 2$^4$ (all possible combinations of codified values +1 and −1); (b) 8 (2$^n$) axial points located at the center and both extreme levels; (c) four central replicates of the central points. The most important parameter for methylparaben degradation was light flux, whereas TiO$_2$ was the least important among the studied factors. The optimal experimental conditions for the highest photocatalytic efficiency of methylparaben estimated by multivariate experimental design were found at: light flux, $5.8 \times 10^{15}$ photons s$^{-1}$ cm$^{-2}$; pH 9; oxygen concentration 18 mg L$^{-1}$; TiO$_2$ loading 2.5 g L$^1$.

Merabet et al. [33] implemented also CCD based on RSM for the modelization and optimization of the photodegradation of indole in the presence of TiO$_2$. The CCD design matrix was built by the statistical combinations of the independent variables of UV irradiance, stirring speed, and indole concentration (20 experimental runs). The experimental results revealed that the influence of UV irradiance was less important than other factors. Finally, by analyzing the contour and 3D response plots, 100% of optimized degradation of target analyte was achieved given by the following values: UV irradiance, 250 W/m$^2$, stirring speed, 536 rpm and initial indole concentration, 10.10 mg/L.

Kansal et al. [34] investigated the influence of catalyst (TiO$_2$) dose, pH and concentration of the oxidant on the photocatalytic degradation of 2,4,6-trichlorophenol in aqueous solutions. In order to study the effect of selected variables a CCD was used and the optimum values were obtained by solving the regression equation and by analyzing the response surface contour plots.

The photocatalytic degradation of cationic dye Alcian Blue 8 GX in the presence of TiO$_2$ P25 was investigated by Caliman et al. [35]. To this end, a 2$^3$ factorial orthogonal design with 15 experimental runs was carried out. This study divulged that the irradiation time had a bigger influence compared to H$_2$O$_2$ concentration and pH. The gradient method was used for the optimization process. The optimum degradation of Alcian Blue 8 GX (100%) was possible by

**Table 3**
Screening the factors by statistical significance test.

| Term | Effect | Coefficient | $t$ | $P$ |
|---|---|---|---|---|
| Mean/interaction | 68.974 | 68.974 | 293.505 | 0.002[a] |
| Curvature | −24.308 | −12.154 | −23.129 | 0.028[a] |
| pH | 3.387 | 1.694 | 7.207 | 0.088 |
| Irradiance | 1.537 | 0.769 | 3.271 | 0.189 |
| Dye concentration | 5.353 | 2.676 | 11.388 | 0.056 |
| $TiO_2$ | 14.288 | 7.144 | 30.399 | 0.021[a] |
| $H_2O_2$ | 6.362 | 3.181 | 13.537 | 0.047[a] |

[a] Significant at 0.05% level; $R^2 = 0.9063$; Adjusted $R^2 = 0.71891$.

the following values: pH 5.26, $H_2O_2$ concentration 191.6 mg/L and time of irradiation-26.3 min.

Fernández et al. [36] investigated the photocatalysis discoloration of Orange II in a photoreactor using $TiO_2$-coated glass rings as immobilized photocatalyst. In this, factorial design was employed with 11 experimental runs (3 center points). $H_2O_2$ concentration and pH were the studied parameters in order to assess the degradation efficiency and a polynomial expression model was developed. This study showed that at low pH, the quantity of $H_2O_2$ added did not critically affect the rate of discoloration to attain full dye decomposition.

Secula et al. [37] examined the photocatalytic decolorization of a simulated dyestuff effluent, containing the azo dye Reactive Black 5. A $2^3$ factorial CCD with 16 experiments runs (6 axial points and 2 center points) were employed for RSM modeling and canonical analysis of the response surface. The experimental factors were: the amount of the $TiO_2$ catalyst and the initial concentrations of the $Fe^{3+}$ ions and $H_2O_2$. By using RSM, 99.30% of color removal was possible under different optimal conditions of process parameters, such as, $TiO_2$, 0.458 g L$^{-1}$, $H_2O_2$, 825.3 mg L$^{-1}$ and $Fe^{3+}$, 40.243 mg L$^{-1}$.

The aim of the research by Cho and Zoh [38] was to apply an experimental design methodology in the optimization of photocatalytic degradation of azo dye (Reactive Red 120). A CCD consisting of 20 experiments was employed for this study. The factors were: dye concentration, $TiO_2$ concentration and irradiance and selected responses were color removal (%) and TOC removal (%). Finally, canonical and ridge analysis of RSM was adopted for optimization. This study showed that irradiance displayed the highest effect for both responses. At pH 7.0, the degradation rate of azo dye was low compared to acidic and alkaline pH. The model accounted for 100% of decolorization of target dye with optimized factors of 1.63 g L$^{-1}$ $TiO_2$, 45.2 mg L$^{-1}$ of reactive dye, and 8.1 mW cm$^{-2}$ of UV irradiance. For TOC, 67.27% of removal was possible by factors optimized at 1.92 g L$^{-1}$ $TiO_2$, 34.7 mg L$^{-1}$ of reactive dye, and 8.5 mW cm$^{-2}$ of UV irradiation.

Other important examples of photocatalytic degradation and design of experiment are stated briefly in Table 1.

## 4. Photocatalytic degradation of CR: a case study

### 4.1. Experimental

Experiments were carried out using $TiO_2$ Degussa P25, as the photocatalyst. Congo red (CR) [dinatirum-3,3′-[[1,1′-biphenyl]-4,4′-diylbis(azo)]bis(4-aminonaphthalin-1-sulfonat), (purity 99%) was purchased from Aldrich and has been used as received.

Irradiation experiments of CR were carried out on stirred aqueous solutions (50 ml, river water) contained in a cylindrical quartz glass UV-reactor. Before irradiation, the suspensions were allowed to stay in the dark for 60 min under stirring, to reach adsorption equilibrium on the semiconductor surface. Irradiation was carried out using a Suntest CPS+ apparatus from Heraeus (Hanau, Germany) equipped with a xenon arc lamp (1500 W) and special glass filters restricting the transmission of wavelengths below 290 nm. Chamber and black panel temperature were regulated by pressurized air cooling circuit and monitored using thermocouples supplied by the manufacturer. The temperature of samples did not exceed 20 °C using tap water cooling circuit for the UV-reactor. To remove $TiO_2$ particles the solution samples were passed through 0.45 μm HA cellulose acetate membrane filters and were further analyzed by monitoring the absorbance at 496 nm using UV–VIS spectrophotometer (Jasco, V-530, Japan).

**Table 4**
Central composite design (CCD) design matrix and results for CR photocatalytic degradation.

| Range and level | | | | | |
|---|---|---|---|---|---|
| Factors | −α | Low (−1) | Middle (0) | High (+1) | +α |
| $TiO_2$ (mg/L) | 575 | 700 | 1000 | 1300 | 1424 |
| $H_2O_2$ (mg/L) | 0.05 | 1.5 | 5 | 8.5 | 9.95 |

| Design matrix | | | | |
|---|---|---|---|---|
| Run | $TiO_2$ | $H_2O_2$ | Degradation % (cal) | Degradation % (Pre) |
| 1 | −1 | −1 | 65.43 | 64.94 |
| 2 | −1 | 1 | 73.45 | 75.93 |
| 3 | 1 | −1 | 75.41 | 72.35 |
| 4 | 1 | 1 | 90.00 | 89.91 |
| 5 | −α | 0 | 59.64 | 60.65 |
| 6 | +α | 0 | 81.26 | 80.84 |
| 7 | 0 | −α | 73.39 | 73.25 |
| 8 | 0 | +α | 87.66 | 88.38 |
| 9 | 0 | 0 | 84.24 | 84.07 |
| 10 | 0 | 0 | 85.75 | 84.07 |
| 11 | 0 | 0 | 84.11 | 84.07 |
| 12 | 0 | 0 | 82.18 | 84.07 |
| 13 | 0 | 0 | 84.05 | 84.07 |

**Table 5**
Sequential model fitting for the CR photocatalytic degradation.

| Sequential model sum of squares | | | | | | |
|---|---|---|---|---|---|---|
| Source | Sum of squares | df | Mean square | F-Value | Prob > F | Remark |
| Mean vs total | 81065.07 | 1 | 81065.07 | | | |
| Linear vs mean | 636.51 | 2 | 318.25 | 9.54 | 0.0048 | |
| 2FI vs linear | 10.79 | 1 | 10.79 | 0.30 | 0.5966 | |
| Quadratic vs 2FI | 312.76 | 2 | 156.38 | 110.65 | ≤0.0001 | Suggested |
| Cubic vs quadratic | 2.78 | 2 | 1.39 | 0.98 | 0.4379 | Aliased |
| Residual | 7.11 | 5 | 1.42 | – | – | |
| Total | 82035.03 | 13 | 6310.39 | – | – | |

| Lack-of-fit tests | | | | | | |
|---|---|---|---|---|---|---|
| Source | Sum of squares | df | Mean square | F-Value | Prob > F | Remark |
| Linear | 327.02 | 6 | 54.50 | 33.93 | 0.0022 | |
| 2FI | 316.23 | 5 | 63.25 | 39.37 | 0.0017 | |
| Quadratic | 3.47 | 3 | 1.16 | 0.72 | 0.5903 | Suggested |
| Cubic | 0.68 | 1 | 0.68 | 0.43 | 0.5495 | Aliased |
| Pure error | 6.43 | 4 | 1.61 | – | – | |

| Model summary statistics | | | | | | |
|---|---|---|---|---|---|---|
| Source | Std. dev. | $R^2$ | Adj. $R^2$ | Pre. $R^2$ | PRESS | Remark |
| Linear | 5.77 | 0.6562 | 0.5875 | 0.5875 | 595.00 | |
| 2FI | 5.99 | 0.6674 | 0.5565 | 0.5565 | 689.13 | |
| Quadratic | 1.19 | 0.9898 | 0.9825 | 0.9825 | 34.70 | Suggested |
| Cubic | 1.19 | 0.9927 | 0.9824 | 0.9824 | 53.84 | Aliased |

## 4.2. Design of experiment

At first, two-level fractional factorial design (resolution III) with five factors was used in order to eliminate unimportant factors before investing time and money in a more elaborate experiment. Eight combinations of all factors and two center points, total 10 experimental runs were carried out (Table 2). Five factors: pH, irradiance, Congo red concentration, $TiO_2$ and $H_2O_2$ concentrations were chosen, according to our previous experience dealing with the photocatalytic processes of micropollutants [9,10,29]. The response was selected as the degradation percentage of the target molecule after 15 min of irradiation. From the analysis of data (Table 3), it can be seen that only $TiO_2$ and $H_2O_2$ have significant impact ($p < 0.05$) on CR degradation. The curvature was also significant, indicating that a higher-order model or response surface study is needed in order to uncover the behavior of the significant factors.

RSM is usually applied following a factorial screening study to explore the region of interest of the factors identified by the preceding study. In order to evaluate the broader effects of the two significant factors (i.e. concentrations of $TiO_2$ and $H_2O_2$) obtained from the screening test, a central composite design (CCD) was used as a RSM. The applied CCD was consisted of 13 experiments ($N = 2^k + 2k + C_0 = 2^2 + 2*2 + 5 = 13$ runs, where $N$ is the total number of experiments required, $k$ is the number of factors $2k$ is axial runs and $C_0$ is center point's runs) including 5 central points. The dis-

tance of the axial points from the center points is called $\alpha$ (alpha). In this study, $\alpha$ value was fixed at 1.414 and can be determined by the multiplication fixed $\alpha$ value with step of factor level and then summation or subtraction of obtained value from the central point. For example, the center point value of $TiO_2$ factor is 1000 and step of level is 300; so $-\alpha$ will be 1000 − (300*1.414) and +$\alpha$ will be 1000 + (300*1.414).

The design matrix is depicted in Table 4. The step-wise model fitting by Design-Expert software (trail version 7, Stat-Ease, Inc., MN) was employed in order to find the best fitted model. The software suggested quadratic model by verifying lack-of-fit and model summary statistics (Table 5). The model adequacy was further checked using ANOVA (Table 6). The Model F-value of 135.86 implies the model is significant. There is only a 0.01% chance that a "Model F-Value" this large could occur due to noise. Values of "Prob > F" less than 0.0500 indicate that model terms are significant. In other words, all factors, in respect of main, interactions and quadratic terms, are significant. The "Lack-of-Fit F-value" of 0.72 implies that the Lack-of-Fit is not significant relative to the pure error. There is a 59.03% chance that a "Lack-of-Fit F-value" this large could occur due to noise. The non-significant lack-of-fit indicates good predictability of the model. The "Pred R-Squared" of 0.9642 is in reasonable agreement with the "Adj R-Squared" of 0.9825 indicating too, a good predictability of the model. Data analysis permitted to obtain a semi-empirical expression in terms of coded values of factors ($\pm\alpha$,

**Table 6**
ANOVA and lack-of-fit (LOF) test for response surface quadratic model of CR photocatalytic degradation.

| Source | Sum of squares | df | Mean square | F-Value | Prob > F | Remarks |
|---|---|---|---|---|---|---|
| Model | 960.06 | 5 | 192.01 | 135.86 | <0.0001 | Significant |
| $TiO_2$ | 407.63 | 1 | 407.63 | 288.43 | <0.0001 | |
| $H_2O_2$ | 228.88 | 1 | 228.88 | 161.95 | <0.0001 | |
| $TiO_2 * H_2O_2$ | 10.79 | 1 | 10.79 | 7.64 | 0.0280 | |
| $TiO_2{}^2$ | 308.72 | 1 | 308.72 | 218.44 | <0.0001 | |
| $H_2O_2{}^2$ | 18.35 | 1 | 18.35 | 12.99 | 0.0087 | |
| Residual | 9.89 | 7 | 1.41 | | | |
| Lack-of-fit | 3.47 | 3 | 1.16 | 0.72 | 0.5903 | Not significant |
| Pure error | 6.43 | 4 | 1.61 | | | |
| Correction total | 969.95 | 12 | | | | |

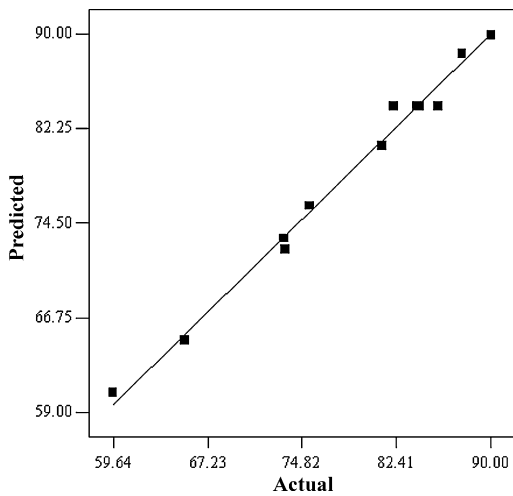**Fig. 1.** Plot of actual vs predicted values.



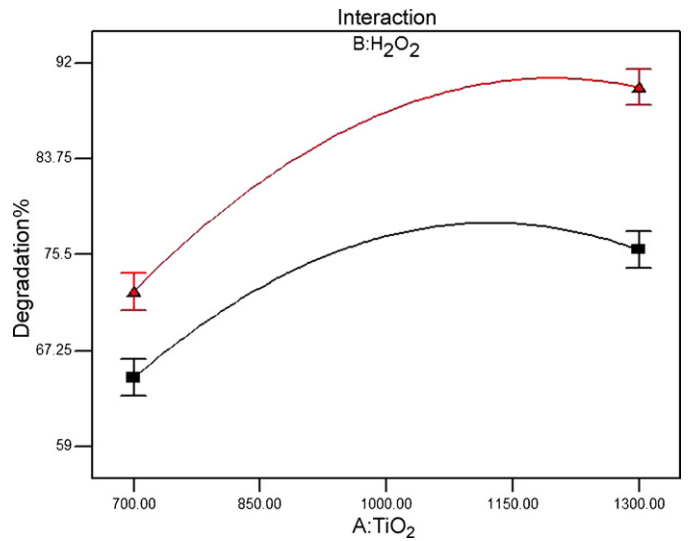**Fig. 3.** Interactions plot for CR photocatalytic degradation.

$\pm 1$, 0), given below

$$\%\text{Degradation} = +84.07 + 7.14 * \text{TiO}_2 + 5.35 * \text{H}_2\text{O}_2$$
$$+ 1.64 * \text{TiO}_2 * \text{H}_2\text{O}_2 - 6.66 * \text{TiO}_2^2$$
$$- 1.62 * \text{H}_2\text{O}_2^2 \quad\quad (6)$$

This model explains perfectly the experimental range studied, as can be seen from the comparison of the graphical representaion of actual *vs* predicted values (Fig. 1). This mathematical expression (Eq. (6)) represents the response factor that is given by the percentage of CR degradation obtained from the decrease of its concentration, after 15 min of photocatalytic reaction.

Figs. 2 and 3 display the plots of individual (main effects) and two-factor interactions effects, respectively, on the CR degradation percent. Analyzing Eq. (3) and taking into consideration only the first-order effects (Fig. 2), the optimum conditions for the photocatalytic degradation of CR seemed to be acquired when $\text{TiO}_2$ ($x_1$) and $\text{H}_2\text{O}_2$ ($x_2$) have a high value, since the highest numerical value of CR degradation ($Y$) corresponds to such conditions. Moreover, it seems that both variables affect, in the same manner, the photocatalytic degradation of CR displaying a high coefficient.

Nevertheless, an excess of $\text{TiO}_2$ ($x_1$), and $\text{H}_2\text{O}_2$ concentration ($x_2$) in the system is adverse for the reaction, bringing out a negative influence on the photocatalytic performance (decreased CR degradation efficiency). The negative coefficients of quadratic terms $\text{TiO}_2^2$, and $\text{H}_2\text{O}_2^2$ (as shown by the second-order effect) in the polynomial expression accounts for this effect.

The overall interaction effects are displayed in Fig. 4; a 3D representation of the polynomial (Eq. (6)) is obtained from the experimental data.

The degradation rate increases proportionally to $\text{TiO}_2$ concentration (up to 1000 mg/L), as expected, confirming the positive influence of the increased number of $\text{TiO}_2$ active sites on the process kinetics. At higher catalyst loading a slight decrease of CR degradation was observed. The availability of active sites increases with catalyst loading, but the light penetration, and hence, the photoactivated volume of the suspension shrinks. Similar observations have also been reported in other studies on various organic substances [64–66].

It is obvious to see (Figs. 2–5) that when the concentration of hydrogen peroxide increases, the degradation rate smoothly
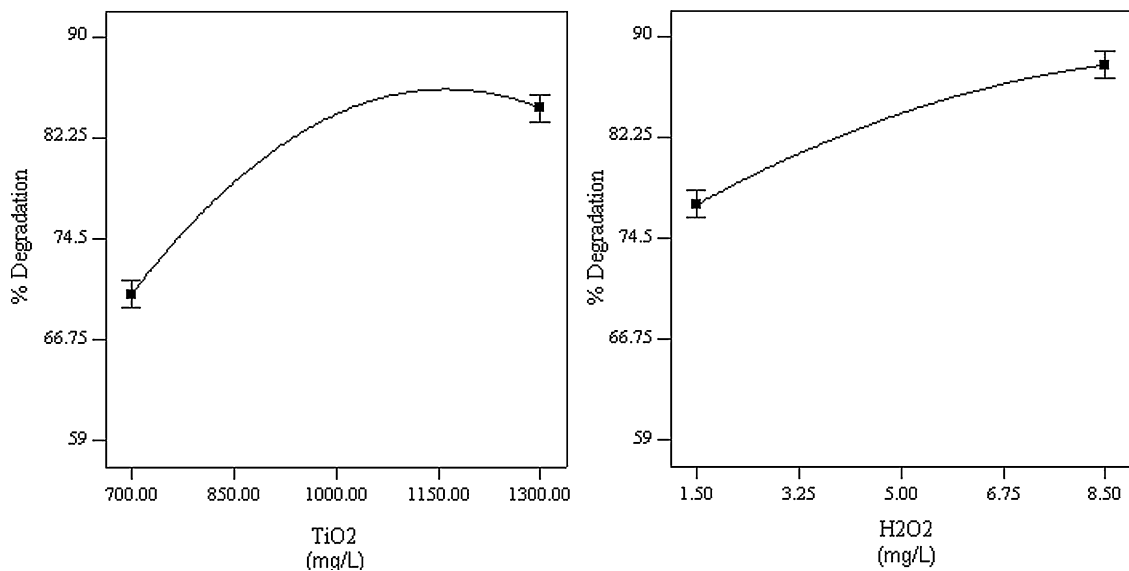


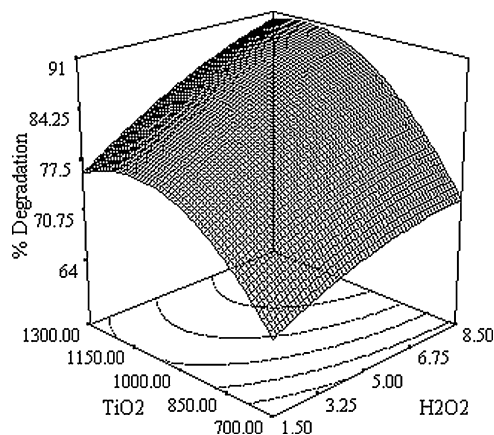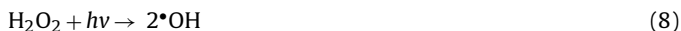**Fig. 2.** Main factors effect for CR photocatalytic degradation.

**Fig. 4.** 3D response surface graph for CR photocatalytic degradation: $TiO_2$ vs $H_2O_2$ concentration.

increases. This positive effect maybe attributed to the inhibition of electron–hole recombination at the semiconductor surface by accepting a photogenerated electron from the conduction band and thus promoting the charge separation (Eq. (7)):

$$e^-_{CB} + H_2O_2 \rightarrow OH^- + {}^\bullet OH \tag{7}$$

The higher reaction rates with increasing $H_2O_2$ can also be attributed to the increase in the concentration of hydroxyl radicals. These radicals are generated by Eq. (7) while on the other hand, peroxide may produce hydroxyl radical directly (Eq. (8)) or by reaction with superoxide anion (Eq. (9)) [67]:

$$H_2O_2 + h\nu \rightarrow 2{}^\bullet OH \tag{8}$$

$$H_2O_2 + O_2{}^- \rightarrow {}^\bullet OH + OH^- + O_2 \tag{9}$$

However, when high concentrations of $H_2O_2$ are used, the degradation efficiency diminishes since it may act as ${}^\bullet OH$ scavenger [68] reducing the amount of radicals available to destroy the CR molecules (Eq. (10)).

$$H_2O_2 + {}^\bullet OH \rightarrow HO_2{}^\bullet + H_2O \tag{10}$$

Although other radicals are produced ($HO_2{}^\bullet$) their oxidation potential is much lower than the ${}^\bullet OH$ species [3].
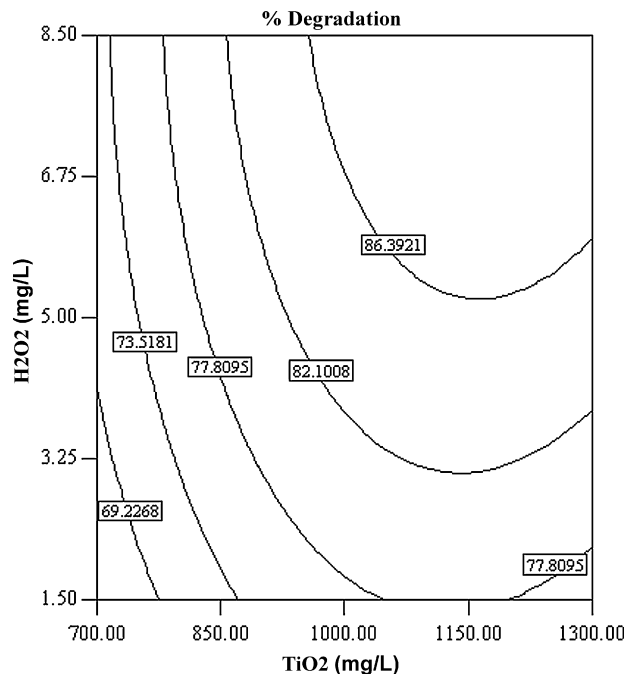


**Fig. 5.** Contour plot for CR photocatalytic degradation: $TiO_2$ vs $H_2O_2$ concentration.

### 4.3. Optimization

After performing a screening of factors and their interactions, the response surface analysis was carried out. Optimization was performed afterwards on the basis of desirability function in order to find the optimal conditions for the degradation of CR.

The numerical optimization of the software has been chosen in order to locate the specific point that maximizes the desirability function. The desired goal was selected by adjusting the weight or importance that might alter the characteristics of a goal. The goal fields for response have five options: none, maximum, minimum, target and within range. The criteria for the optimization of all studied factors in correspondence with degradation % are shown in Table 7. From the ANOVA (Table 6), it has been seen that the main effects of $TiO_2$ and $H_2O_2$ were significant, therefore,
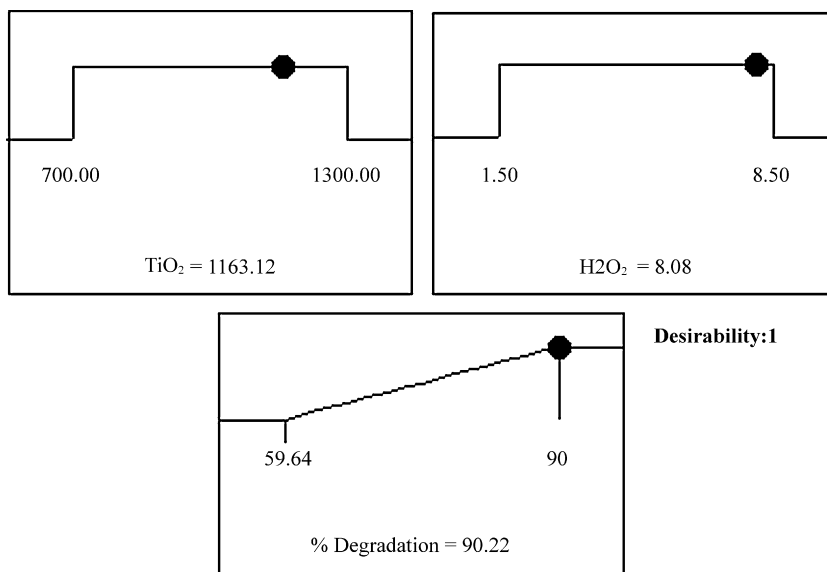


**Fig. 6.** Desirability ramp for numerical optimization.

**Table 7**
Optimization of the individual responses ($d_i$) in order to obtain the overall desirability response ($D$).

| Name | Goal | Lower limit | Upper limit | Lower weight | Upper weight | Importance |
|---|---|---|---|---|---|---|
| $TiO_2$ | Is in range | 700 | 1300 | 1 | 1 | 3 |
| $H_2O_2$ | Is in range | 1.5 | 8.5 | 1 | 1 | 3 |
| Degradation % | Maximize | 59.64 | 90 | 1 | 1 | 5 |

these factors were assigned as 'within range' with corresponding 'importance' 3. As higher degradation % is usually preferred for such studies, 'importance' 5 was assigned as the maximum goal. The lower limit and upper limit values of all responses are taken from the CCD design levels. Our main objective was to maximize the degradation yield with recalculating all responsible factors by using desirability functions. By using all above described settings and boundaries, the software optimized 90.22% degradation of CR with calculating the optimized model factors of $TiO_2$ at 1163 mg/L and $H_2O_2$ at 8.1 mg/L, respectively (Fig. 6). Finally, for their validation, duplicate confirmatory experiments were conducted using the optimized parameters for CR degradation (89.66%). The results are closely related with the data obtained from optimization analysis using desirability function, indicating that CCD design in combination with desirability function could be effectively used to optimize the degradation of CR from aqueous solution.

Our results are in agreement with a recent study by Erdemoglu et al. [69]. Photodegradation of Congo red in aqueous solutions by hydrothermally synthesized anatase $TiO_2$ with nanocrystalline size (8 nm) has shown that nano-$TiO_2$ catalysts can easily degrade 20 mg L$^{-1}$ CR dye after visible irradiation for 30 min. A similar study revealed that the shape of $TiO_2$ nanocrystals significantly affected the photocatalytic activities of CR [70].

$TiO_2$/UV-based photocatalysis was not only able to decolorize but also to fully oxidize the dyes, giving rise to a complete mineralization of carbon into $CO_2$ [71]. Other advanced oxidation processes as UV/$H_2O_2$, resulted in poor mineralization efficiency and needed long irradiation periods [72].

### 4.4. Toxicity assessment

The toxicity of CR solution and of aqueous samples collected at different irradiation times was examined by Microtox Model 500 Toxicity Analyzer. The detailed procedure of analysis was described elsewhere [29]. The initial toxicity of CR solution (0 h
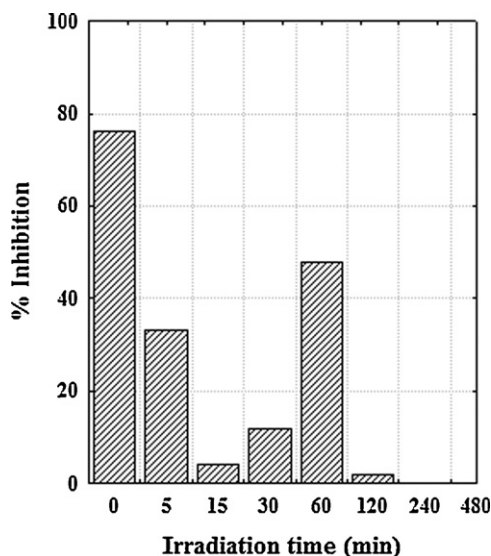
of irradiation) showed an inhibition of 76%. As the photocatalytic treatment proceeds, the toxicity of the solution rapidly decreases and reaches a value of 4% inhibition, at 15 min (Fig. 7). Thereafter, inhibition % increases (60 min, inhibition of 48%) but remains lower compared to CR initial toxicity. These observations clearly demonstrate that transformation products, more toxic than CR are formed, while synergistic effects among them are also considered. At higher irradiation times, the toxicity is decreased until complete detoxification of the irradiated solution is achieved.

## 5. Conclusion

Response surface methodology (RSM) is nowadays, a promising as well as a powerful tool for multivariate optimization through sequential experimentation. Several researchers have already been using various RSM approaches to explain optimization process. This review article explicates the RSM theory, and provides several applications to highlight the importance of DOE in the field of photocatalytic processes. Finally, an example of CR dye photocatalytic degradation with application of multivariate optimization again suggests that RSM approach is applicable as a chemometric tool that can provide systematic satisfactory results.

**Fig. 7.** Inhibition (%) of the luminescence of bacteria *Vibrio fischeri* as a function of the photocatalytic treatment time.

## References

[1] W.C. Paterlini, R.F. Pupo Nogueira, Multivariate analysis of photo-Fenton degradation of the herbicides tebuthiuron, diuron and 2,4-D, Chemosphere 58 (2005) 1107–1116.
[2] M.J. Farre, X. Domenech, J. Pera, Assessment of photo-Fenton and biological treatment coupling for Diuron and Linuron removal from water, Water Res. 40 (2006) 2533–2540.
[3] J.H. Ramirez, C.A. Costa, L.M. Madeira, Experimental design to optimize the degradation of the synthetic dye Orange II using Fenton's reagent, Catal. Today 107–108 (2005) 68–76.
[4] I.K. Konstantinou, T.A. Albanis, Photocatalytic transformation of pesticides in aqueous titanium dioxide suspensions using artificial and solar light: intermediates and degradation pathways, Appl. Catal. B: Environ. 42 (2003) 319–335.
[5] A. Fujishima, K. Hashimoto, T. Watanabe, TiO₂ Photocatalysis, Fundamentals and Applications, Bkc Inc., Tokyo, 1999.
[6] J.M. Herrmann, J. Disdier, P. Pichat, S. Malato, J. Blanco, TiO2-based solar photocatalytic detoxification of water containing organic pollutants. Case studies of 2,4-dichlorophenoxyaceticacid (2,4-D) and of benzofuran, Appl. Catal. B: Environ. 17 (1998) 15–23.
[7] S. Esplugas, D.M. Bila, L.G.T. Krause, M. Dezotti, Ozonation and advanced oxidation technologies to remove endocrine disrupting chemicals (EDCs) and pharmaceuticals and personal care products (PPCPs) in water effluents, J. Hazard. Mater. 149 (2007) 631–642.
[8] C. Zwiener, F.H. Frimmel, Oxidative treatment of pharmaceuticals in water, Water Res. 34 (2000) 1881–1885.
[9] V.A. Sakkas, P. Calza, C. Medana, A.E. Villioti, C. Baiocchi, E. Pelizzetti, T. Albanis, Heterogeneous photocatalytic degradation of the pharmaceutical agent salbutamol in aqueous titanium dioxide suspensions, Appl. Catal. B: Environ. 77 (2007) 135–144.
[10] P. Calza, V.A. Sakkas, C. Medana, C. Baiocchi, A. Dimou, E. Pelizzetti, T. Albanis, Photocatalytic degradation study of diclofenac over aqueous TiO₂ suspensions, Appl. Catal. B: Environ. 67 (2006) 197–205.
[11] T. Lundstedt, E. Seifert, L. Abramo, B. Thelin, A. Nyström, J. Pettersen, R. Bergman, Experimental design and optimization, Chemom. Intell. Lab. Syst. 42 (1998) 3–40.
[12] R.H. Myers, D.C. Montgomery, Response Surface Methodology: Process and Product Optimization Using Designed Experiments, second ed., Wiley, New York, 2002.
[13] J. Goupy, Methods for Experimental Design. Principles and Applications for Physicists and Chemists, Elsevier, Amsterdam, 1993.
[14] S.L.C. Ferreira, R.E. Bruns, H.S. Ferreira, G.D. Matos, J.M. David, G.C. Brandão, E.G.P. da Silva, L.A. Portugal, P.S. dos Reis, A.S. Souza, W.N.L. dos Santos, Box–Behnken design: an alternative for the optimization of analytical methods, Anal. Chim. Acta 597 (2007) 179–186.

[15] S.L.C. Ferreira, W.N.L. dos Santos, C.M. Quintella, B.B. Neto, J.M. Bosque-Sendra, Doehlert matrix: a chemometric tool for analytical chemistry—review, Talanta 63 (2004) 1061–1067.

[16] J. Goupy, What kind of experimental design for finding and checking robustness of analytical methods? Anal. Chim. Acta 544 (2005) 184–190.

[17] M.A. Bezerra, R.E. Santelli, E.P. Oliveira, L.S. Villar, L.A. Escaleira, Response surface methodology (RSM) as a tool for optimization in analytical chemistry, Talanta 76 (2008) 965–977.

[18] S.L.C. Ferreira, R.E. Bruns, E.G.P. da Silva, W.N.L. dos Santos, C.M. Quintella, J.M. David, J.B. de Andrade, M.C. Breitkreitz, I.C.S.F. Jardim, B.B. Neto, Statistical designs and response surface techniques for the optimization of chromatographic systems, J. Chromatogr. A 1158 (2007) 2–14.

[19] C. Stalikas, Y. Fiamegos, V. Sakkas, T. Albanis, Developments on chemometric approaches to optimize and evaluate microextraction, J. Chromatogr. A 1216 (2009) 175–189.

[20] J. Gabrielsson, N.-O. Lindberg, T. Lundstedt, Multivariate methods in pharmaceutical applications, J. Chemom. 16 (2002) 141–160.

[21] S. Wold, M. Sjöström, R. Carlson, T. Lundstedt, S. Hellberg, B. Skagerberg, C. Wikström, J. Öhman, Multivariate design, Anal. Chim. Acta 191 (1986) 17–32.

[22] M. Boeniger, Carcinogenecity and metabolism of azo dyes, especially those derived from benzidine, USDHHS (NIOSH) Tech. Rep. (1980) 80–119.

[23] S. Maiti, S. Purakayastha, B. Ghosh, Production of low-cost carbon adsorbents from agricultural wastes and their impact on dye adsorption, Chem. Eng. Commun. 195 (2008) 386–403.

[24] G.E.P. Box, J.S. Hunter, W.G. Hunter, Statistics for Experimenters: Design, Innovation, and Discovery, second ed., Wiley Interscience, New Jersey, 2005.

[25] G.W. Oehlert, Design and Analysis of Experiments: Response Surface Design, W.H. Freeman and Company, New York, 2000.

[26] E.C. Harrington, The desirability function, Ind. Qual. Cont. 21 (1965) 494–498.

[27] G. Derringer, R. Suich, Simultaneous optimization of several response variables, J. Qual. Technol. 12 (1980) 214–219.

[28] C.A. Emilio, J.F. Magallanes, M.I. Litter, Chemometric study on the TiO$_2$-photocatalytic degradation of nitrilotriacetic acid, Anal. Chim. Acta 595 (2007) 89–97.

[29] P. Calza, V.A. Sakkas, A. Villioti, C. Massolino, V. Boti, E. Pelizzetti, T. Albanis, Multivariate experimental design for the photocatalytic degradation of imipramine: determination of the reaction pathway and identification of intermediate products, Appl. Catal. B: Environ. 84 (2008) 379–388.

[30] B.K. Korbahti, M.A. Rauf, Response surface methodology (RSM) analysis of photoinduced decoloration of toludine blue, Chem. Eng. J. 136 (2008) 25–30.

[31] M.A. Rauf, N. Marzouki, K. Bahadir, Korbahti, Photolytic decolorization of Rose Bengal by UV/H$_2$O$_2$ and data optimization using response surface method, J. Hazard. Mater. 159 (2008) 602–609.

[32] Y. Lin, C. Ferronato, N. Deng, F. Wu, J.-M. Chovelon, Photocatalytic degradation of methylparaben by TiO$_2$: multivariable experimental design and mechanism, Appl. Catal. B: Environ. 88 (2008) 32–41.

[33] S. Merabet, D. Robert, J.-V. Weber, M. Bouhelassa, S. Benkhanouche, Photocatalytic degradation of indole in UV/TiO$_2$: optimization and modelling using response surface methodology (RSM), Environ. Chem. Lett. 7 (2009) 45–49.

[34] S.K. Kansal, M. Singh, D. Sud, Optimization of photocatalytic process parameters for the degradation of 2,4,6-trichlorophenol in aqueous solutions, Chem. Eng. Commun. 194 (2007) 787–802.

[35] A.F. Caliman, C. Cojocaru, A. Antoniadis, I. Poulios, Optimized photocatalytic degradation of Alcian Blue 8 GX in the presence of TiO$_2$ suspensions, J. Hazard. Mater. 144 (2007) 265–273.

[36] J. Fernández, J. Kiwi, J. Baeza, J. Freer, C. Lizama, H.D. Mansilla, Orange II photocatalysis on immobilised TiO$_2$: effect of the pH and H$_2$O$_2$, Appl. Catal. B: Environ. 48 (2004) 205–211.

[37] M.S. Secula, G.D. Suditu, I. Poulios, C. Cojocaru, I. Cretescu, Response surface optimization of the photocatalytic decolorization of a simulated dyestuff effluent, Chem. Eng. J. 141 (2008) 18–26.

[38] I.-H. Cho, K.-D. Zoh, Photocatalytic degradation of azo dye (*Reactive Red 120*) in TiO$_2$/UV system: optimization and modeling using a response surface methodology (RSM) based on the central composite design, Dyes Pigment 75 (2007) 533–543.

[39] A. Danion, C. Bordes, J. Disdier, J.-Y. Gauvrit, C. Guillard, P. Lantéri, N. Jaffrezic-Renault, Optimization of a single TiO$_2$-coated optical fiber reactor using experimental design, J. Photochem. Photobiol. A: Chem. 168 (2004) 161–167.

[40] S.A.V. Eremia, D. Chevalier-Lucia, G.-L. Radu, J.-L. Marty, Optimization of hydroxyl radical formation using TiO$_2$ as photocatalyst by response surface methodology, Talanta 77 (2008) 858–862.

[41] J. Fu, Q. Wu, Statistical designs of experiments for photocatalytic process of Acid Blue 7 dye wastewater by nano TiO$_2$, Taiyangneng Xuebao/Acta Energiae Solaris Sinica 29 (2008) 152–157.

[42] H.-L. Liu, Y.-R. Chiou, Optimal decolorization efficiency of Reactive Red 239 by UV/TiO$_2$ photocatalytic process coupled with response surface methodology, Chem. Eng. J. 112 (2005) 173–179.

[43] C. Lizama, J. Freer, J. Baeza, H.D. Mansilla, Optimized photodegradation of reactive blue 19 on TiO$_2$ and ZnO suspensions, Catal. Today 76 (2002) 235–246.

[44] S. Merabet, M. Schneider, D. Robert, S. Benkhanouche, M. Bouhelassa, J.V. Weber, Optimization of the indole photodegradation on supported TiO$_2$: influences of temperature, concentration, TiO$_2$ amount and flow rate, Water Sci. Technol. 58 (2008) 549–554.

[45] M. Bosco, M.S. Larrechi, Rapid and quantitative evaluation of the effect of process variables on the kinetics of photocatalytic degradation of phenol using experimental design techniques and parallel factor (PARAFAC) analysis, Anal. Bioanal. Chem. 390 (2008) 1203–1207.

[46] M. Sleiman, D. Vildozo, C. Ferronato, J.-M. Chovelon, Photocatalytic degradation of azo dye Metanil Yellow: optimization and kinetic modeling using a chemometric approach, Appl. Catal. B: Environ. 77 (2007) 1–11.

[47] S. Ray, J.A. Lalman, N. Biswas, Using the Box–Benkhen technique to statistically model phenol photocatalytic degradation by titanium dioxide nanoparticles, Chem. Eng. J. 150 (2008) 15–24.

[48] C.-H. Wu, K.-S. Huang, J.-M. Chern, Decomposition of acid dye by TiO$_2$ thin films prepared by the sol–gel method, Ind. Eng. Chem. Res. 45 (2006) 2040–2045.

[49] E.C. Catalkaya, F. Kargi, Effects of operating parameters on advanced oxidation of diuron by the Fenton's reagent: a statistical design approach, Chemosphere 69 (2007) 485–492.

[50] J. Fu, Y. Zhao, Q. Wu, Optimising photoelectrocatalytic oxidation of fulvic acid using response surface methodology, J. Hazard. Mater. 144 (2007) 499–505.

[51] C.A. Emilio, M.I. Litter, J.F. Magallanes, Semiempirical modeling with application of artificial neural networks for the photocatalytic reaction of ethylenediaminetetraacetic acid (EDTA) over titanium oxide (TiO$_2$), Helv. Chim. Acta 85 (2002) 799–813.

[52] M.B. Kasiri, H. Aleboyeh, A. Aleboyeh, Modeling and optimization of heterogeneous photo-Fenton process with response surface methodology and artificial neural networks, Environ. Sci. Technol. 42 (2008) 7970–7975.

[53] K. Bahadir, M.A. Korbahti, Rauf, Application of response surface analysis to the photolytic degradation of Basic Red 2 dye, Chem. Eng. J. 138 (2008) 166–171.

[54] K. Bahadir, M.A. Korbahti, Rauf, Determination of optimum operating conditions of carmine decoloration by UV/H$_2$O$_2$ using response surface methodology, J. Hazard. Mater. 161 (2009) 281–286.

[55] S.-M. Lee, Y.-G. Kim, I.-H. Cho, Treatment of dyeing wastewater by TiO$_2$/H$_2$O$_2$/UV process: experimental design approach for evaluating total organic carbon (TOC) removal efficiency, J. Environ. Sci. Health Part A: Toxic/Hazard. Subst. Environ. Eng. 40 (2005) 423–436.

[56] C. Betianu, F.A. Caliman, M. Gavrilescu, I. Cretescu, C. Cojocaru, I. Poulios, Response surface methodology applied for Orange II photocatalytic degradation in TiO$_2$ aqueous suspensions, J. Chem. Technol. Biotechnol. 83 (2008) 1454–1465.

[57] F. Ay, E.C. Catalkaya, F. Kargi, A statistical experiment design approach for advanced oxidation of direct red azo-dye by photo-Fenton treatment, J. Hazard. Mater. 162 (2009) 230–236.

[58] W. Gernjak, M. Fuerhacker, P. Fernández-Ibañez, J. Blanco, S. Malato, Solar photo-fenton treatment process parameters and process control, Appl. Catal. B: Environ. 64 (2006) 121–130.

[59] R. Molina, F. Martiῐnez, J.A. Melero, D.H. Bremner, A.G. Chakinala, Mineralization of phenol by a heterogeneous ultrasound/Fe-SBA-15/H$_2$O$_2$ process: multivariate study by factorial design of experiments, Appl. Catal. B: Environ. 66 (2006) 198–207.

[60] M. Rios-Enriquez, N. Shahin, C. Durán-De-Bazúa, J. Lang, E. Oliveros, S.H. Bossmann, et al., Optimization of the heterogeneous Fenton-oxidation of the model pollutant 2,4-xylidine using the optimal experimental design methodology, Solar Energy 77 (2004) 491–501.

[61] M.C. Yeber, C. Soto, R. Riveros, J. Navarrete, G. Vidal, Optimization by factorial design of copper (II) and toxicity removal using a photocatalytic process with TiO$_2$ as semiconductor, Chem. Eng. J., in press.

[62] R.A. Palominos, M.A. Mondaca, A. Giraldo, G. Peñuela, M. Pérez-Moya, H.D. Mansilla, Photocatalytic oxidation of the antibiotic tetracycline on TiO$_2$ and ZnO suspensions, Catal. Today, in press.

[63] J. Nieto, J. Freer, D. Contreras, R.J. Candal, E.E. Sileo, H.D. Mansilla, Photocatalyzed degradation of flumequine by doped TiO$_2$ and simulated solar light, J. Hazard. Mater. 155 (2008) 45–50.

[64] K. Nohara, H. Hidaka, E. Pelizzetti, N. Serpone, Processes of formation of NH$^{3+}$ and NO$^{3-}$ ions during the photocatalyzed oxidation of N-containing compounds at the titania/water interface, J. Photochem. Photobiol. A: Chem. 102 (1997) 265–272.

[65] C.M. So, M.Y. Cheng, J.C. Yu, P.K. Wong, Degradation of azo dye Procion Red MX-5B by photocatalytic oxidation, Chemosphere 46 (2002) 905–912.

[66] K. Nohara, H. Hidaka, E. Pelizzetti, N. Serpone, Dependence on chemical structure of the production of NH$^{4+}$ and/or NO$^{3-}$ ions during the photocatalyzed oxidation of nitrogen-containing substances at the titania/water interface, Catal. Lett. 36 (1996) 115–118.

[67] A. Duran, J.M. Monteagudo, Solar photocatalytic degradation of reactive blue 4 using a Fresnel lens, Water Res. 41 (2007) 690–698.

[68] J.M. Monteagudo, M. Carmona, A. Duran, Photo-Fenton-assisted ozonation of p-Coumaric acid in aqueous solution, Chemosphere 60 (2005) 1103–1110.

[69] S. Erdemoglu, S.K. Aksub, F. Sayılkan, B. Izgi, M. Asilturk, H. Sayılkan, F. Frimmel, S. Gucer, Photocatalytic degradation of Congo red by hydrothermally synthesized nanocrystalline TiO$_2$ and identification of degradation products by LC–MS, J. Hazard. Mater. 155 (2008) 469–476.

[70] R.K. Wahi, W.W. Yu, Y. Liu, M.L. Mejia, J.C. Falkner, W. Nolte, V.L. Colvin, Photodegradation of Congo Red catalyzed by nanosized TiO$_2$, J. Mol. Catal. A: Chem. 242 (2005) 48–56.

[71] H. Lachheb, E. Puzenat, A. Houas, M. Ksibi, E. Elaloui, C. Guillard, J.-M. Herrmann, Photocatalytic degradation of various types of dyes (Alizarin S, Crocein Orange G, Methyl Red, Congo Red, Methylene Blue) in water by UV-irradiated titania, Appl. Catal. B: Environ. 39 (2002) 75–90.

[72] U. Balia, E. Catalkaya, F. Sengul, Photodegradation of reactive black 5, direct red 28 and direct yellow 12 using UV, UV/H$_2$O$_2$ and UV/H$_2$O$_2$/Fe$^{2+}$: a comparative study, J. Hazard. Mater. B114 (2004) 159–166.